PHYSICAL REVIEW B VOLUME 32, NUMBER 12 15 DECEMBER 1985

Surface quenching of optically generated carriers in thin-film hydrogenated amorphous silicon: Picosecond transient-grating experiments

Vincent J. Newell, Todd S. Rose, and M. D. Fayer
Department of Chemistry, Stanford University, Stanford, California 94305
(Received 1 July 1985)

Subnanosecond-timescale transient-grating experiments are used to investigate the dynamics of optically generated charge carriers in thin-film hydrogenated amorphous silicon (a-Si:H) at room temperature. By examining the time dependence of the transient-grating signal as a function of fringe spacing for small fringe spacing, the diffusion constant in the plane of the film ($D_{||}$) is determined. At large fringe spacing, the grating decay becomes independent of fringe spacing and is highly nonexponential. The functional form and rate of the large-fringe-spacing decay change with sample thickness. A model for the effect of surface quenching on the transient-grating decay is presented. The calculations are in good agreement with the data and yield a diffusion constant ($D_{\perp}$) for motion perpendicular to the thin-film plane. $D_{\perp}=0.4\times10^{-2}$ cm^2/sec, while $D_{||}=1.0\times10^{-2}$ cm^2/sec.

I. INTRODUCTION

In this paper we present a room-temperature experimental study of the transport and surface quenching of optically generated charge carriers in thin-film hydrogenated amorphous silicon (a-Si:H). At low temperature (4.2 K), in high-quality samples, the principal mechanism for carrier quenching is radiative recombination.[1] Nonradiative processes such as Auger recombination and tunneling to defects play only a minor role.[1] However, it has been suggested[2] that surface effects play an important role at higher temperatures (77 K). Rehm *et al.*[2(a)] examined the effects of sample thickness and wavelength (optical penetration depth) on the decay time of the luminescence. They found dramatic effects when the sample thickness or the optical penetration depth fell below 0.3 μm.

In the experiments presented below, we use a picosecond transient-grating technique[3] to investigate carrier transport in 0.33- and 0.16-μm samples of a-Si:H. The application of the picosecond transient-grating technique is based on earlier investigations of excitation[4] and exciton[5] transport in molecular crystals. The transient-grating experiment works in the following manner [see Fig. 1(a)]. A picosecond-timescale pulse of light is split in two. The paths of the resulting pulses are arranged to have a known angle between them and to intersect simultaneously in the sample. Interference between the two coherently related pulses creates an optical fringe pattern in the sample such that the intensity of light varies sinusoidally in the beam-overlap region. The interference fringe spacing is determined by the angle between the beams and by the wavelength of the light.

The wavelength of the excitation pulses is tuned above the band gap. Electron-hole pairs are excited and relax to band-edge localized states. The relaxation occurs on a timescale that is short compared to the time required for transport over macroscopic distances.[6] The localized carriers will have the same spatial distribution as the sinusoidal optical interference pattern, i.e., there will be a continuous oscillatory variation in the concentration of electron-hole pairs. After a suitable time delay, a probe pulse (which may differ in wavelength from the exciting pulses) is directed into the sample along a third path. The probe pulse will experience an inhomogeneous optical medium resulting from alternating regions of high and low concentrations of electron-hole pairs. The separated charges associated with an electron-hole pair perturbs the electron distribution in the local environment, and therefore changes the index of refraction. The result is that the spatial variation in the number density of electron-hole pairs produces a spatially periodic variation in the index of refraction. Thus, the probe pulse encounters a diffraction grating (phase grating) which causes it to diffract into one or more orders [see Fig. 1(a)]. Phase gratings have been previously observed in experiments on crystalline silicon.[7] The diffracted pulse leaves the sample along a unique direction.

In the experiments described below, the grating wave vector is in the plane of the a-Si:H sample. For small fringe spacing (~1 μm), carrier transport dominates the grating decay. Migration will move carriers from areas of high concentration (grating peaks) to areas of low concentration (grating nulls). Thus, the motion will fill in the grating nulls and deplete the peaks. Destruction of the grating pattern by spatial redistribution of the carriers over macroscopic distances will lead to a decrease in the intensity of the diffracted probe pulse as the probe delay time is increased. For a small fringe spacing, time dependence of the grating signal is directly determined by the rate of transport. As the fringe spacing is increased, the decay of the signal arising from spatial transport is slowed because it takes longer for carriers to move from grating peaks to grating nulls.

For sufficiently large fringe spacing, the decay of the grating due to in-plane transport will become negligible compared to other decay pathways. The large-fringe-spacing time-dependent signal is independent of fringe spacing; therefore, the dynamics of other processes can be

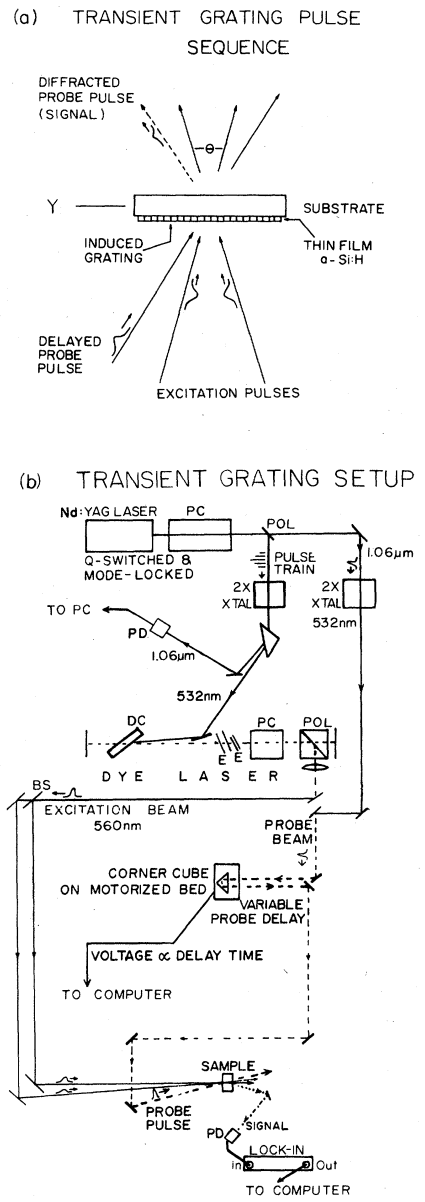

FIG. 1. (a) Transient-grating pulse sequence. Two excitation pulses are crossed simultaneously in a thin film of a-Si:H at an angle θ. They optically interfere and absorption produces a spatially periodic variation in the concentration of photoexcited carriers which mimics the optical fringe pattern. This periodic pattern of carriers act as a phase grating that Bragg-diffracts a variably delayed probe pulse. The diffracted beam is the signal. Note that the a-Si:H layer is not drawn to scale. (b) Transient-grating experimental setup. A single picosecond 1.06-μm pulse is selected from a pulse train produced by an acousto-optically Q-switched and mode-locked Nd:YAG laser. The single pulse is then frequency-doubled to 532 nm to produce the probe pulse. The remaining ir pulse train is doubled and used to synchronously pump a dye laser. The dye laser is cavity-dumped to yield single pulses at 560 nm. These pulses are beam-split and made to cross in the sample to produce the transient grating. Time delay of the probe is achieved with a motorized delay line. DC, dye cell; POL, polarizer; PC, Pockels cell; BS, beam splitter; E, étalon; PD, photodiode.

investigated. In experiments involving electronic excited-state gratings, the large-fringe-spacing decay is due to the exponential decay of the excited states,[3-5] and the transient-grating signal decay is a single exponential. In the experiments described below, the large-fringe-spacing decay is highly nonexponential and depends on the thickness of the thin film. A model is presented which relates the large-fringe-spacing decay to carrier diffusion and quenching at the thin-film surfaces. The model provides a good description of the nonexponential time dependence and thickness dependence of the signal in terms of a diffusion constant $D_\perp$ for transport perpendicular to the plane of the thin film. $D_\perp$ is distinct from the diffusion constant $D_\parallel$ measured in the thin-film plane at small fringe spacing. We find $D_\parallel = 1.0\times10^{-2}$ cm^2/sec and $D_\perp = 0.4\times10^{-2}$ cm^2/sec. The results demonstrate that surface quenching is the dominant decay path for photogenerated carriers at room temperature and that the surface recombination occurs on the first encounter with the surface region.

II. MATHEMATICAL FORMULATION

First consider a system in which the photogenerated carriers undergo diffusive transport but do not decay either by surface quenching or other recombination processes. The optical interference pattern produces electron-hole pairs in the medium such that the initial spatial distribution along the grating axis (y direction) is given by[3-5]

$$N(y,0)=\tfrac{1}{2}[1+\cos(\Delta y)]\ , \tag{1}$$

where

$$\Delta = 2\pi/d\ , \tag{2}$$

and d, the grating fringe spacing, is given by

$$d=\frac{\lambda}{2\sin(\theta/2)}\ . \tag{3}$$

In Eq. (3), λ is the wavelength of the excitation pulses (in air) and θ is the angle between them (in air) [see Fig. 1(a)]. A variable-time-delay probe pulse is diffracted off the induced grating. The diffracted probe is monitored as a function of time delay between the probe and the excitation pulses.

The change in signal, as a function of time (i.e., the decay of the grating), results from motion of the carriers along the grating axis. The appropriate diffusion equation is

$$\frac{\partial N(y,t)}{\partial t}=D_\parallel\frac{\partial^2 N(y,t)}{\partial y^2}\ . \tag{4}$$

In Eq. (4), $D_\parallel$ is the diffusion constant parallel to the grating wave vector. $N(y,t)$ describes the distribution of carriers along the grating axis at time t. The solution of the above equation for the initial condition given by Eq. (1) is

$$N(y,t)=\tfrac{1}{2}[1+e^{-\Delta^2 D_\parallel t}\cos(\Delta y)]\ . \tag{5}$$

The time-dependent grating signal is proportional to the

square of the difference, γ, in the carrier concentrations at the grating peaks and nulls.[8,9] The time dependence of γ is a function of the fringe spacing, and therefore the angle between the beams, θ [see Eqs. (2) and (3)],

$$\gamma(t,\theta)=N(0,t)-N(d/2,t)=e^{-(\Delta^2 D_{||}t)} . \quad (6)$$

Consequently, the time-dependent signal is

$$S(t,\theta)=A\gamma(t,\theta)^2=Ae^{-Kt} , \quad (7)$$

where A, a time-independent constant, describes the strength of the signal and depends on beam geometries, laser intensities, and other experimental factors. For small θ, the decay constant K is given by

$$K=2\Delta^2 D_{||}=(8\pi^2/\lambda^2)\theta^2 D_{||} . \quad (8)$$

It is seen that for diffusive transport along the grating axis, the signal decays exponentially at a rate which depends directly on the diffusion constant in the grating-wave-vector direction. In the absence of carrier-decay processes, the diffusion constant can be obtained from one grating-decay measurement at a particular value of θ. In practice, however, it is generally better to evaluate the decay as a function θ. If transport is responsible for the grating decay, then a plot of K versus θ^2 should yield a straight line. The diffusion constant is obtained from the slope of the line. This is the procedure employed below.

In real systems the grating decays due to processes other than diffusion along the grating-wave-vector direction. The time dependence of the grating arising from these other processes is independent of θ. The total signal can be written as

$$S(t,\theta)=Ae^{-Kt}f(t) . \quad (9)$$

In the limit that θ is very small (large fringe spacing), the exponential term is constant and the signal becomes angle independent,

$$S(t,\theta\approx 0)=S_0(t)=Af(t) . \quad (10)$$

For the excited-state gratings previously reported, the small-angle decay is dominated by the single-exponential decay of the excited states;[3,8] $f(t)=\exp(-2t/\tau)$, where τ is the excited-state lifetime. Here we will present a model in which $f(t)$ is not exponential and is determined by surface quenching of the electron-hole pairs. Regardless of the form of $f(t)$, the angle-dependent part of the signal, $S_\theta(t,\theta)$, which yields the in-plane diffusion constant $D_{||}$, can be obtained by dividing Eq. (9) by Eq. (10), i.e.,

$$S_\theta(t,\theta)=\frac{S(t,\theta)}{S_0(t)}=e^{-Kt} . \quad (11)$$

At large fringe spacing, the signal is fringe-spacing independent. However, the signal is nonexponential and is dependent on the sample thickness. To account for this we present equations which allow us to calculate the time-dependent probability that carriers initially located at various distances from the samples surface or interface have interacted with either of the sample boundaries. The sample boundaries are located at $x=0$ and $x=s$. The initial distribution of electron-hole pairs is given by Beer's law. The model assumes that an electron-hole pair is quenched upon reaching a surface, and that no other bulk recombination pathways are significant.

Consider a point in the sample x_0 at which carriers are generated by optical absorption. The time-dependent probability density distribution along the x axis due to the carriers generated at x_0 is

$$P(x,x_0,t)=\frac{1}{2(\pi D_\perp t)^{1/2}}\exp[-(x-x_0)^2/4D_\perp t] . \quad (12)$$

$D_\perp$ is the diffusion coefficient for the direction perpendicular to the plane of the thin film (x axis). The probability that carriers originating at x_0 have quenched by diffusing to one of the boundaries at $x=0$ and $x=s$ is

$$P_Q(x_0,t)=\frac{1}{2}\left[\operatorname{erfc}\left[-\frac{x_0}{2(D_\perp t)^{1/2}}\right]+\operatorname{erfc}\left[\frac{s-x_0}{2(D_\perp t)^{1/2}}\right]\right] , \quad (13)$$

where erfc is the error-function complement. The probability that carriers with an initial distribution throughout the depth of the sample, $f(x_0)$, have reached one of the boundaries is

$$P_Q(t)=\tfrac{1}{2}\int_0^s f(x_0)\left[\operatorname{erfc}\left[-\frac{x_0}{2(D_\perp t)^{1/2}}\right]+\operatorname{erfc}\left[\frac{s-x_0}{2(D_\perp t)^{1/2}}\right]\right]dx_0 . \quad (14)$$

The distribution function is normalized between the boundaries 0 and s. For a Beer's-law initial distribution assumed here,

$$f(x_0)=\frac{\alpha e^{-\alpha x_0}}{1-e^{-\alpha s}} , \quad (15)$$

where α is the absorption coefficient.

The time development of the transient-grating signal, $S_0(t)$, is proportional to the square of the peak-null difference in the density of carriers.[8,9] In the large-fringe-spacing case, as described by this model, the number of carriers in the nulls remain constant in time, and for equal-amplitude excitation pulses the constant is equal to zero. Therefore, the signal is proportional to the square of the carriers remaining in the sample, i.e.,

$$S_0(t)=A[1-P_Q(t)]^2=A\left\{1-\frac{\alpha}{2(1-e^{-\alpha s})}\int_0^s e^{-\alpha x_0}\left[\operatorname{erfc}\left[-\frac{x_0}{2(D_\perp t)^{1/2}}\right]+\operatorname{erfc}\left[\frac{s-x_0}{2(D_\perp t)^{1/2}}\right]\right]dx_0\right\}^2 . \quad (16)$$

Equation (16) displays a nonexponential time decay which is dependent on the sample thickness, provided s is on the order of the Beer's length, $1/\alpha$. For $s \gg 1/\alpha$, the carriers are generated so far from the back surface of the sample that the signal decay at relatively short times is completely dominated by quenching at the front surface. However, when $s \approx 1/\alpha$, the time dependence is a sensitive function of s. This behavior is displayed in the data reported below.

The model described above calculates the probability of interacting with the surface as the fraction of spreading Gaussians which is past the interfaces. Actually, this is a first-passage problem, i.e., the time-dependent probability that carriers encounter the surface for the first time should be calculated. However, the difference between the procedure used here and a first-passage calculation will be small.

III. EXPERIMENTAL PROCEDURES

The experimental system is illustrated schematically in Fig. 1(b). The laser is a cw-pumped, acousto-optically Q-switched and mode-locked Nd:YAG (YAG denotes yttrium aluminum garnet) system which produces 1.06-μm pulse trains at 400 Hz.[10] A single pulse of 80 ps duration and ~ 40 μJ in energy is selected by a Pockels cell. The selected ir pulse is then frequency-doubled by a CD*A (cesium dideuterium arsenate) crystal to produce a 532-nm, 60-psec, 15-μJ TEM_{00} pulse. The remaining 1.06-μm pulse train is also frequency-doubled and used to synchronously pump a dye laser which produces a 560-nm, 30-psec, 10-μJ dye-laser pulse.[8]

The 560-nm single pulse is passed through a 50% beam splitter and the resulting two pulses are recombined to form the interference pattern at the sample. The 532-nm single pulse is used as the probe. A retroreflector is drawn along a precision optical rail by a motor which provides continuous scanning of the probe delay. A ten-turn potentiometer, also driven by the motor, provides a voltage proportional to the probe delay. The diffracted signal is spatially and spectrally filtered and is detected by a large-area photodiode and lock-in amplifier. The output of the lock-in amplifier and the voltage proportional to the probe-time delay are digitalized and stored by a computer for subsequent analysis.

The a-Si:H samples were provided by Dr. R. D. Wieting of Arco Solar Corporation. The samples were prepared by standard glow-discharge procedures on Suprasil substrates. The substrate temperature was held at 200 °C. A silane pressure of 1 Torr was used and the growth rate was a few Å/sec. Several substrates were coated in each run. The results presented below did not vary for different samples from the same coating run, nor did they vary for different spots on a given sample. Samples with different thicknesses show significant differences, as discussed in the next section. The samples were mounted in air. Spot sizes were 300 μm for the excitation beams and 230 μm for the probe beam. The beams were attenuated to approximately 2 μJ per beam. For the power levels employed to obtain the results presented below, no damage to the samples occurred during the tens of minutes required to conduct a single experiment.

IV. RESULTS AND DISCUSSION

Figure 2 shows the time-dependent decay of the transient-grating signal for two different spacings. The sample is 0.33 μm thick. The top trace is for a fringe spacing of 6.3 μm. For fringe spacings larger than 5 μm the grating decay is fringe-spacing independent. This decay defines $S_0(t)$ [Eq. (10)] for this sample. The lower trace is for a fringe spacing of 1.0 μm. This decay is substantially faster than the upper trace due to carrier transport from grating peaks to grating nulls. The function $S_\theta(t,\theta)$, which characterizes the in-plane transport ($D_{||}$), is obtained from the data using Eq. (11). Figure 3(a) shows a plot of K versus θ^2. The points fall on a straight line and, from Eq. (8), yield a diffusion constant $D_{||} = 1.0 \times 10^{-2}$ cm^2/sec.

These data were reproducible for various spots on the same sample and various samples made in the same deposition run, provided the excitation and probe pulses were sufficiently attenuated. With the full laser power and ~ 300-μm spot sizes, permanent gratings were burned into the sample. After excitation with full power, extremely intense, time-independent diffraction occurred even when the excitation beams were blocked. Examination of the sample showed that a striped pattern had been produced. It appeared as if the a-Si:H had been removed from the sample. In the data presented, the beams were attenuated until no damage of the samples occurred. The decay curves were also checked to see if the time dependence was affected by power. For the energies used in the experiments, the data were power independent. The effect of repetition rate was also tested, and the decays were found to be independent of repetition rate. This indicates the absence of long-lived species (>1 msec), which are important at very low temperatures.[1]

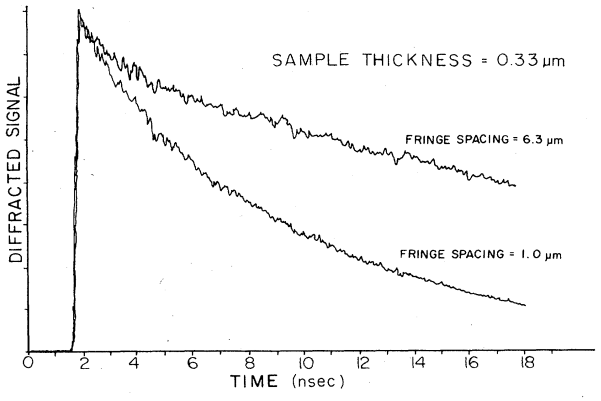

FIG. 2. Transient-grating signal decay for the 0.33-μm-thick sample at two different fringe spacings. The upper decay curve for 6.3-μm fringe spacing is highly nonexponential and is dominated by surface quenching of the photoexcited carriers. The decay for 6.3-μm fringe spacing is in the large-fringe-spacing limit, where the shape of the decay is determined by sample thickness and is insensitive to the fringe spacing. The lower decay curve at 1.0-μm-fringe spacing is faster due to diffusion of carriers in the plane of the sample from the grating peaks to the nulls, which destroys the grating pattern.

important at very low temperatures.[1]

Figure 3(b) shows a plot of K versus θ^2 for a 0.16-μm sample. Again, the data fall on a straight line and yield a value of $D_{||}=0.8\times10^{-2}$ cm^2/sec. While this is very close to the $D_{||}$ obtained for the thicker sample, it falls somewhat outside of the range of experimental uncertainty. Whether this difference is due to the different sample thicknesses or arises because the samples were made in different deposition runs is presently unclear.

Figures 4(a) and 4(b) show decay curves taken on the 0.33- and 0.16-μm samples, respectively, with a 6.3-μm fringe spacing. At this fringe spacing, the decays are fringe-spacing independent. The decays in the two samples are clearly different. These decays are nonexponential. Previously, experiments similar to these were conducted on samples with a thickness of 0.6 μm.[11] The data were interpreted in terms of a single exponential lifetime at large fringe spacing for samples which had not been previously illuminated to induce the Staebler-Wronski effect.[12] (The authors indicate almost an-order-of-magnitude variation in their measured lifetime values.) However, there is no reason to believe that a single lifetime would characterize the electron-hole—pair decay. This is certainly not the case at low temperature, where radiative recombination exhibits a power-law time dependence.[1]

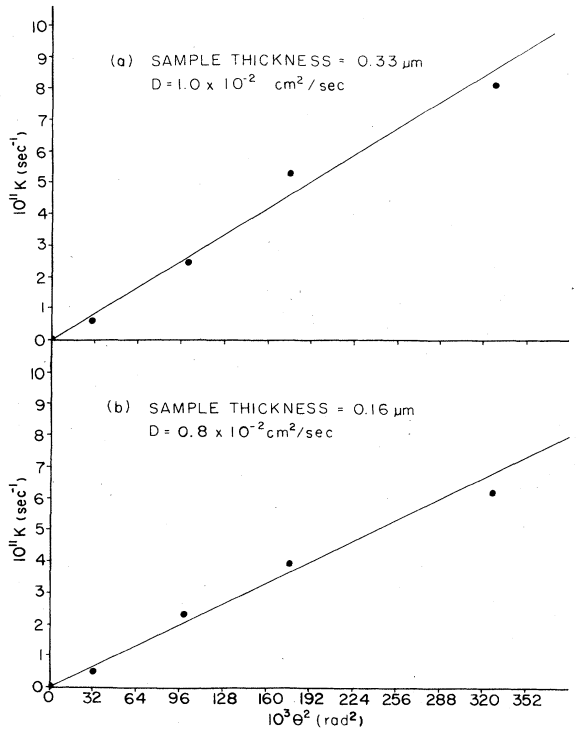

FIG. 3. (a) K vs θ^2 for a 0.33-μm-thick a-Si:H using Eq. (11). For diffusive transport, the points should fall on a straight line. The slope equals $8\pi^2 D_{||}/\lambda^2$ and therefore yields the value of the diffusion constant, $D_{||}=1.0\times10^{-2}$ cm^2/sec. (b) K vs θ^2 for the 0.16-μm-thick film. For this sample, $D_{||}=0.8\times10^{-2}$ cm^2/sec.

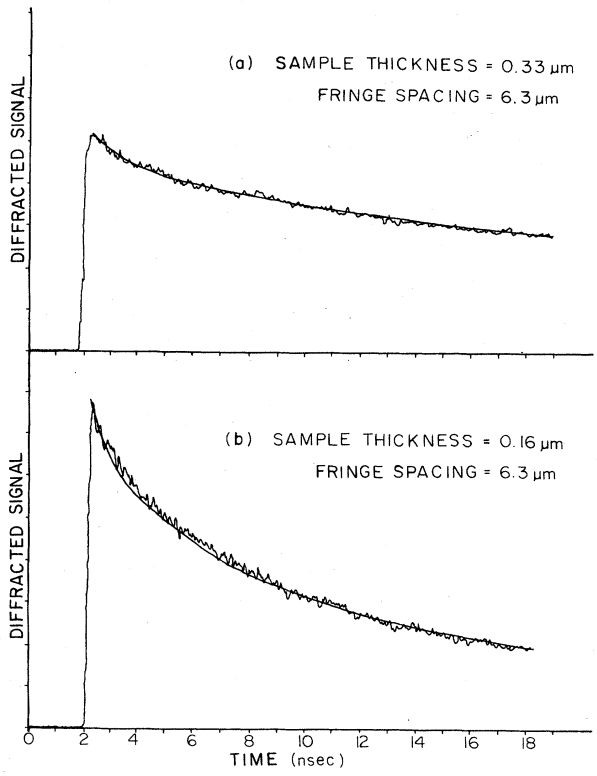

FIG. 4. The data in 4(a) and (b) are for the same fringe spacing (6.3 μm) but different sample thickness, 0.33 and 0.16 μm, respectively. The decay in the thicker sample is highly nonexponential and substantially slower than the decay in the thinner sample. The solid curve in (a) was fitted to the data using the surface-quenching model, Eq. (16), and one adjustable parameter, $D_\perp$. A value of $D_\perp=0.4\times10^{-2}$ cm^2/sec gave the best fit. The solid curve in (b) was calculated without adjustable parameters using the $D_\perp$ value obtained from the data in (a). The very good agreement between the theoretical curves and the data demonstrates that the model for the dynamics of surface quenching is essentially correct.

We propose a model for the large-fringe-spacing decay, i.e., surface quenching, which explains both the nonexponential shapes of the curves and the change in shape with sample thickness. Electron-hole pairs migrate to the vicinity of the surface where they undergo a radiationless recombination process. The nonexponential form of the decays is due to the distributions of transit times from the bulk of a sample to the surfaces. The thicker sample has a broader distribution of transit times than the thinner sample, resulting in a differently shaped decay curve. The solid lines through the data were calculated using the simple diffusion model described in Sec. II. The data in Fig. 4(a) were fitted to Eq. (16) with one adjustable parameters $D_\perp$. The best value for $D_\perp$ was 0.4×10^{-2} cm^2/sec. The solid curve through the data in Fig. 4(b) was calculated without adjustable parameters using the $D_\perp$ value obtained from the fit in Fig. 4(a). The quantitative agreement between the data and the calculated curves is strong support for the basic idea that surface quenching is the

dominant carrier-recombination process in thin-film *a*-Si:H at room temperature.

In these experiments the maximum average intensity used, ~ 6 W/cm^2, is sufficient to produce the Staebler-Wronski effect.[12] No changes in the data were observed when the beams were attenuated such that the average intensity was less than 2 W/cm^2, nor did we observe any change in the time-dependent decays as the illumination time increased. Komuro *et al.* report the appearance of a fast (~ 100 psec) decay component for samples which had been irradiated for $2\frac{1}{2}$—4 h with broadband visible and uv light of intensity 0.3 W/cm^2. We did not observe any time dependence which could not be accounted for by the transport and surface-quenching model presented above. The relatively short illumination times (~ 20 min) and lack of uv irradition could account for the absence of a fast component. Furthermore, the samples used in these experiments are considerably thinner than the samples of Komuro *et al.*, emphasizing the role of surfaces in carrier recombination.

While the agreement between the model calculation and the data is quite good, it is important not to overinterpret the meaning of these results. Transport to the surface can be characterized by a macroscopic diffusion constant. However, the microscopic mode of transport is almost certainly not strictly diffusive. The fact that $D_\perp$ is smaller than $D_{||}$ can be qualitatively explained by invoking band bending near the surface. Presumably the transport of holes to surface-quenching sites is the rate-limiting step.[13] The band-edge localized hole states increase in energy as the surface is approached. At room temperature there is enough thermal energy available to move up hill, but at a reduced rate. The net result is that transport to the surface is slower than transport in the plane. If this qualitative picture is correct, or for similar scenarios, the motion of the carriers at the microscopic level is not characterized by a single diffusion constant. Transport toward the surface slows down as the surface is approached.

The macroscopic surface-quenching model presented here works because it embodies the essential features of the physical situation. There is a distribution of starting locations in the bulk of the material. This results in a wide distribution of transit times to the surface. The transit time to the surface is the rate-limiting step in the surface quenching. While transport is probably not strictly diffusive, it can be approximately characterized by an effective diffusion constant, $D_\perp$.

ACKNOWLEDGMENTS

We would like to thank Dr. Robert Wieting, Arco Solar Corporation, for providing us with the *a*-Si:H samples and for many stimulating and informative conversations pertaining to this work. We would also like to thank Professor Nathan Lewis, Stanford University, for discussions which aided this research. This work was supported by the National Science Foundation, Division of Materials Research (Grant No. DMR-84-16343), and by Department of Energy, Office of Basic Energy Sciences (Grant No. DE-FG03-84ER13251). We would also like to thank the Stanford National Science Foundation Center for Materials Research for Central Facility Support which aided this research.

[1]R. A. Street, Adv. Phys. **30**, 593 (1981); R. A. Street, in *Semiconductors and Semimetals,* edited by J. I. Pankove (Academic, New York, 1984) Vol. 21, P. B, p. 197.

[2](a) W. Rehm, R. Fischer, and J. Beichler, Appl. Phys. Lett. **37**, 445 (1980); (b) R. A. Street and D. K. Biegelsen, in *The Physics of Hydrogenated Amorphous Silicon II,* Vol. 56 of *Topics in Applied Physics,* edited by J. D. Joannopoulos and G. Lucovsky (Springer, New York, 1984), p. 195; R. A. Street and J. C. Knights, Philos. Mag. B **43**, 1091 (1981).

[3]H. J. Eichler, Opt. Acta **246**, 631 (1977).

[4]J. R. Salcedo, A. E. Siegman, D. D. Dlott, and M. D. Fayer, Phys. Rev. Lett. **41**, 131 (1978).

[5]T. S. Rose, R. Righini, and M. D. Fayer, Chem. Phys. Lett. **106**, 13 (1984).

[6]E. O. Gobel and W. Grandszus, Phys. Rev. Lett. **48**, 1277 (1982); Z. Vardeny, J. Strait, and J. Tauc, in *Picosecond Phenomena III,* edited by K. B. Eisenthal, R. M. Hochstrasser, W. Kaiser, and A. Laubereau (Springer, Berlin, 1982), p. 372.

[7]J. P. Woerdman, Phillips Res. Rep. Suppl. No. 7 (1971).

[8]K. A. Nelson, R. Casalegno, R. J. D. Miller, and M. D. Fayer, J. Chem. Phys. **77**, 1144 (1982).

[9]R. F. Loring and S. Mukamel, J. Chem. Phys. (to be published).

[10]D. J. Kuizenga, D. W. Phillion, T. Lund, and A. E. Siegman, Opt. Commun. **9**, 221 (1973).

[11]S. Komuro, Y. Aoyagi, Y. Segawa, S. Namba, A. Masuyama, H. Okamoto, and Y. Hamakawa, Appl. Phys. Lett. **42**, 79 (1983); **42**, 807 (1983).

[12]D. L. Staebler and C. R. Wronski, Appl. Phys. Lett. **31**, 292 (1977).

[13]C. Tsang and R. A. Street, Phys. Rev. B **19**, 3027 (1979).